

Electronic Supplementary Information

A TICT based NIR-fluorescent probe for Human Serum Albumin: a pre-clinical diagnosis in blood serum

Shahi Imam Reja, Imran A. Khan, Vandana Bhalla and Manoj Kumar*

Department of Chemistry, UGC Sponsored Centre for Advanced Studies-1, Guru Nanak Dev University, Amritsar, Punjab, India. E-mail: mksharmaa@yahoo.co.in

Page No. Contents

S-2: Experimental: Materials and reagents, estimation of human serum albumin (HSA) in human blood serum and denaturation of proteins.

S-2 to S-4: Synthesis of probe **3** and ^1H , ^{13}C NMR and Mass spectra of probe **3**.

S-5: UV-vis and fluorescence spectra of probe **3** in HEPES buffer.

S-5: UV-vis spectrum in presence of human serum albumin and Normalized fluorescence spectrum of probe **3** in different solvent systems.

S-5: Fluorescence spectra of probe **3** (10.0 μM) in the presence of different viscosity and calculated λ_{fl} for different concentration of glycerol: H_2O systems.

S-6: HOMO-LUMO energy level of probe **3** for ground state and excited state.

S-6: Theoretical Oscillator strength vs percentage of glycerol and Tables of structural properties and electrochemical properties at various concentration of glycerol.

S-7 to S-8: Limit of detection graph and calculation.

S-8: Fluorescence selectivity bar diagram of probe **3** (10.0 μM) in the presence of various analytes.

S-9: Fluorescence lifetime decay profiles of probe **3** in the presence HSA (15 μM) in H_2O buffered with HEPES, $\text{pH} = 7.4$.

S-9: Job's plot for determining the stoichiometry and displacement of probe **3** from **HSA-3** complex by addition of different site-specific drugs.

S-10: Different docking poses with HSA and BSA.

S-11: HOMO-LUMO using the ground state configuration in QM/MM protocol in HSA-probe and BSA-probe complexes.

S-11 to S-13: Output results of QM/MM calculation of both the proteins with the respective probe.

S-14 to S-15: Results with the trimmed proteins of the both BSA and HSA

S-15 to S-16: Results of the trimmed protein optimization.

S-16: Different states of **HSA-3** complex used for the calculation of reorganization energy.

S-17: Different states of **BSA-3** complex used for the calculation of reorganization energy and calculation of reorganisation energy values for both **HSA-3** and **BSA-3** complex.

S-18: HSA level in different human blood samples using probe **3** and clinical test.

Experimental Section

General information

All reagents were purchased from Aldrich and were used without further purification. HPLC grade solvent was used in UV-vis and fluorescence studies. Human serum albumin (HSA), bovine serum albumin (BSA), glutathione reductase (GSSR), hemoglobin, trypsin, lysozyme and other amino acids were purchased from Sigma-Aldrich. UV-vis spectra were recorded on a SHIMADZU UV-2450 spectrophotometer, with a quartz cuvette (path length 1 cm). The fluorescence spectra were recorded with a SHIMADZU 5301 PC spectrofluorimeter. ^1H and ^{13}C NMR spectra were recorded on a Bruker Avance III HD 500 MHz spectrophotometer using CD_3CN as solvent. Data are reported as follows: chemical shift in ppm (d), multiplicity (s = singlet, d = doublet, t = triplet, m = multiplet, br = broad singlet), coupling constants J (Hz). Protein Sensing Experiments was carried out followed by previous report.

Estimation of HSA in Human Blood Serum

Blood samples were collected from university health center, healthy donors and hypertension patients into a blood collecting tube using sterilized syringe and needle. Serum on the top portion is then pipetted out and used for the analysis. The HSA content in blood serum was estimated with probe **3** by standard addition method. A calibration plot was prepared by measuring the emission maximum at 680 nm upon addition of different concentration of HSA into the probe **3**. The unknown concentration of HSA protein in the blood serum was calculated from the calibration curve by diluting the serum sample appropriately within the linear range.

Synthesis of probe 3:

To a solution of *N,N*-dimethylaminocinnamaldehyde **1** (100 mg, 0.5714 mmol) with 1,2,3,3-tetramethyl-3H-indol-1-ium **2** (206 mg, 0.6857 mmol) in acetic anhydride (20 ml) and sodium acetate reflux for 12 hrs. Then, water (8 mL) was added to the reaction mixture to quench the reaction. The solvent was removed under reduced pressure to give the crude product which was further recrystallization in ethanol gave the desired product as bluish

coloured solid. ^1H NMR (CD_3CN , 500 MHz) δ (ppm) = 1.74 (s, 6 H), 3.12 (s, 6 H), 3.81 (s, 3 H), 6.66 (d, $J = 10$ Hz, 1 H), 6.83 (d, $J = 5$, 2 H), 7.23-7.18 (m, 1 H), 7.54-7.52 (m, 1 H), 7.64-7.56 (m, 5 H), 7.66 (d, $J = 5$ Hz, 1 H), 8.14 (d, $J = 5$ Hz, 1 H). ^{13}C NMR (CD_3CN , 125 MHz, $\delta = \text{ppm}$) = 25.770, 32.904, 39.462, 51.274, 110.543, 112.269, 113.491, 122.562, 123.067, 128.164, 129.044, 131.841, 142.206, 142.691, 152.752, 153.495, 156.485, 179.936. TOF MS ES^+ , data for: $\text{C}_{23}\text{H}_{27}\text{N}_2^+$ Found: 331.2128 (M^+); calculated: 331.2169 (M^+).

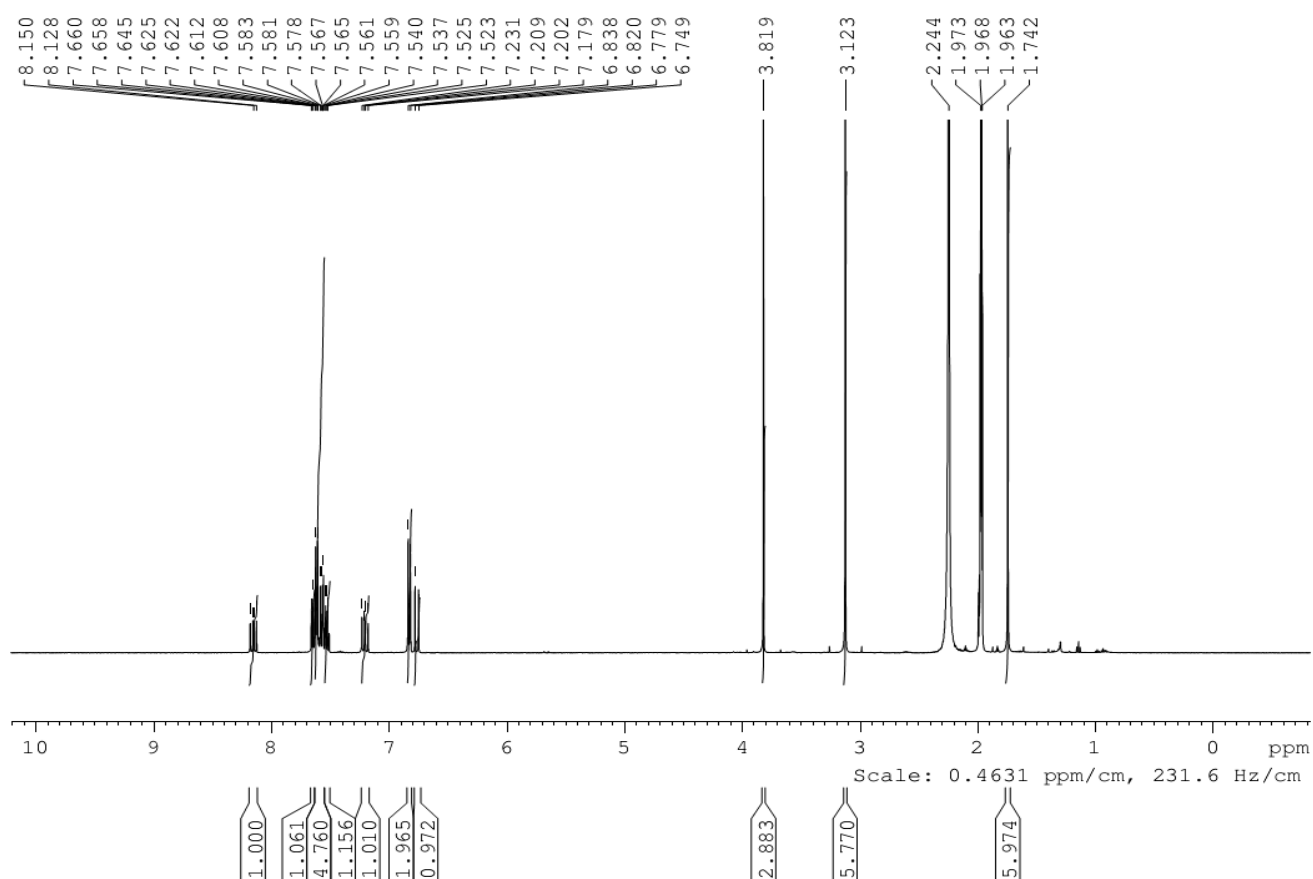


Figure S1: ^1H NMR of probe **3** in CD_3CN

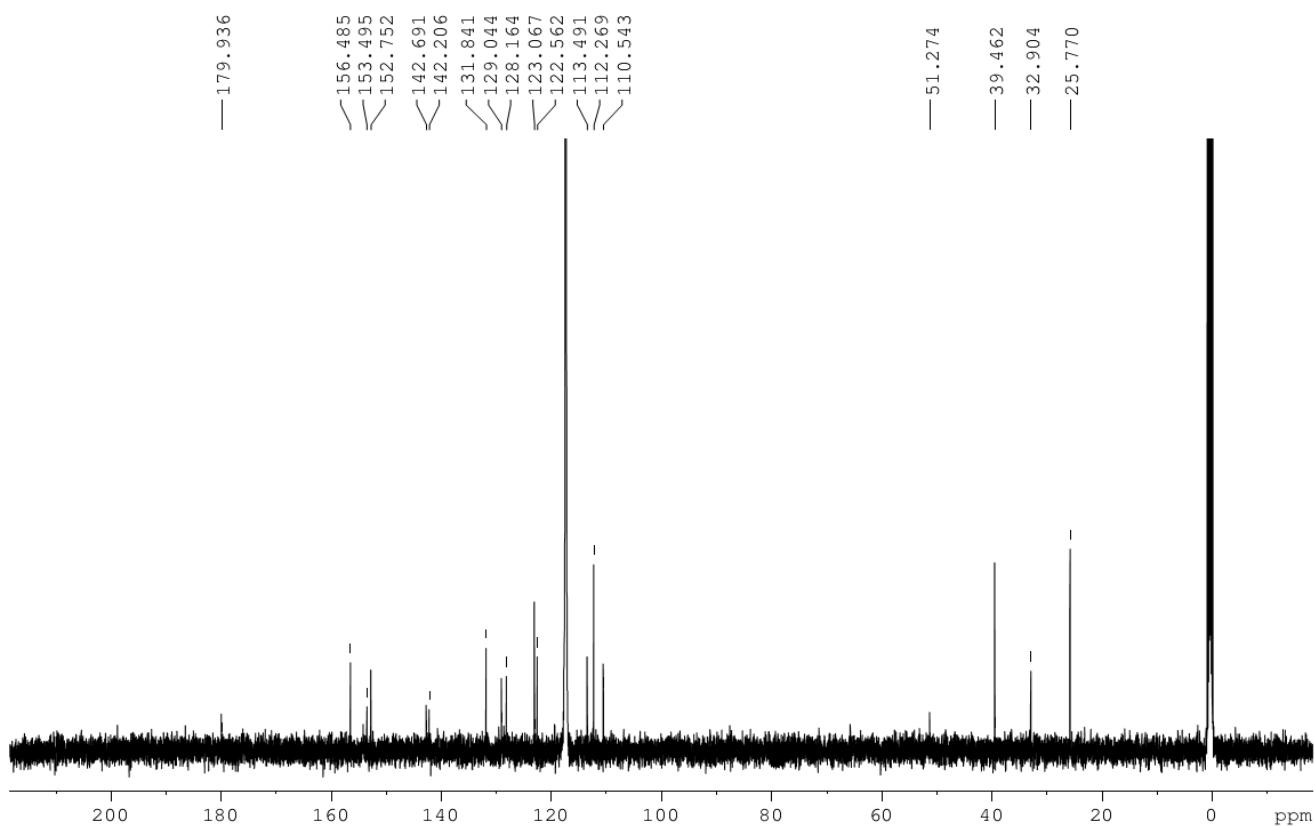


Figure S2: ^{13}C NMR of probe **3** in CD_3CN

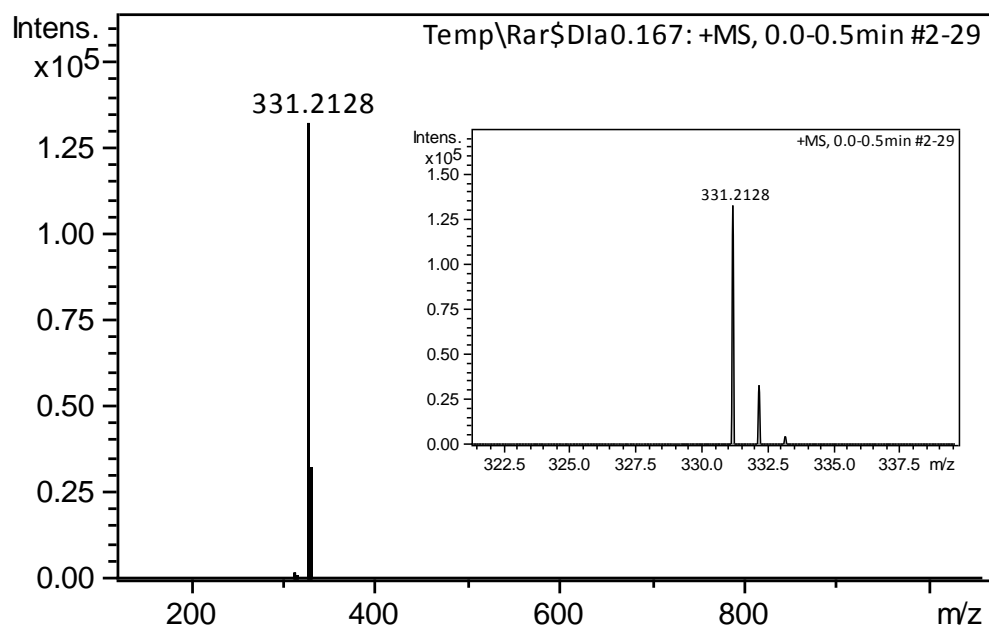


Figure S3: Mass spectra of probe **3** (inset expand the region)

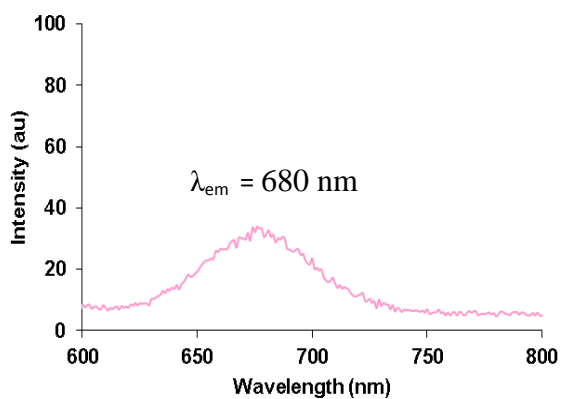


Figure S4a: Fluorescence spectra of probe **3** in H₂O buffered with HEPES, pH = 7.4.

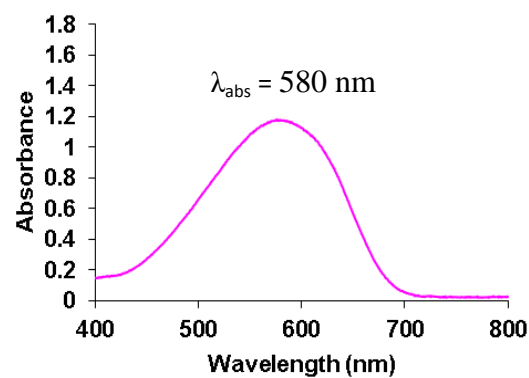


Figure S4b: UV-vis spectra of probe **3** in H₂O buffered with HEPES, pH = 7.4.

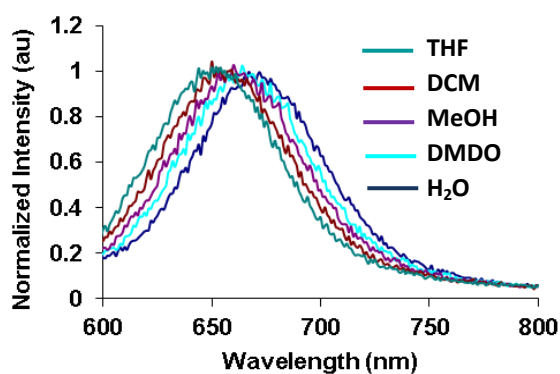


Figure S5: Normalized fluorescence spectrum of probe **3** in different solvent systems at $\lambda_{\text{ex}} = 550$ nm and $\lambda_{\text{em}} = 680$ nm.

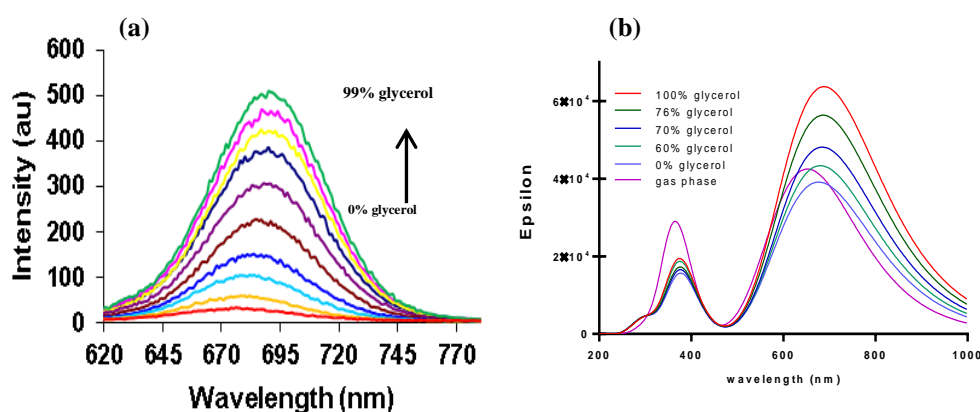


Figure S6: (a) Fluorescence spectra of probe **3** (10.0 μM) in the presence of different viscosity in H₂O/glycerol fraction. $\lambda_{\text{ex}} = 550$ nm; (b) Calculated λ_{fl} for different concentration of glycerol:H₂O systems.

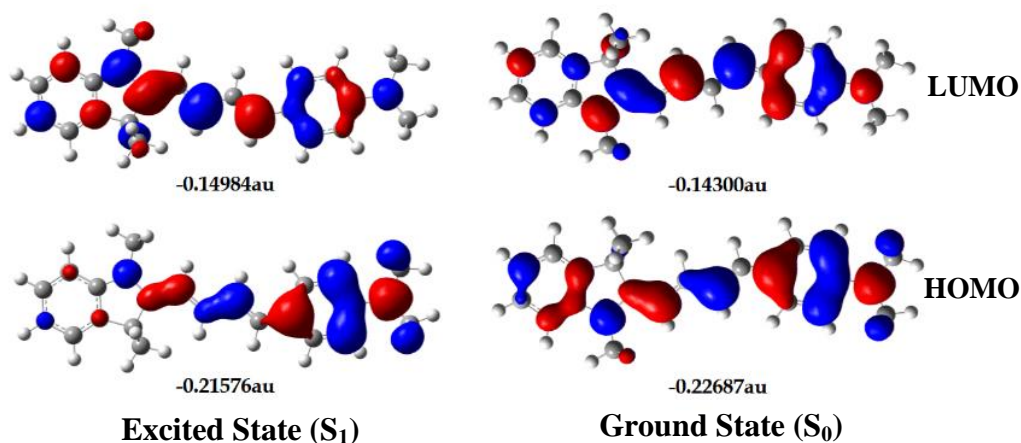


Figure S7: HOMO-LUMO energy level of probe **3** for ground state and excited state.

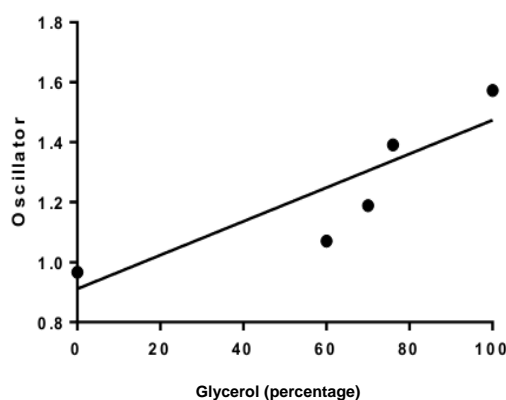


Figure S8: Theoretical Oscillator strength vs percentage of glycerol

Table S1. Theoretical Oscillator strength (CAM-B3LYP 6-311G*) versus concentration of glycerol

Entry	Glycerol (percentage)	f	Dielectric constant	$\lambda_{\text{Flourescence}} (\lambda_{\text{abs}})$
1	0.	0.9659	78.50	676.67
2	60.	1.0705	60.00	680.3
3	70.	1.1885	55.60	684.41
4	76.	1.3915	50.60	686.3
5	100.	1.5729	40.10	688.39
6	Gas phase	1.0489	-	652.23 (520.89)

Table S1.1. Table of structural properties and electrochemical properties at various concentration of glycerol

	0% glycerol	60% glycerol	70% glycerol	76% glycerol	glycerol
C ₁ -C ₄	1.43323	1.43769	1.43453	1.43552	1.43882
C ₄ -C ₃	1.38957	1.38526	1.38827	1.38731	1.38423
C ₃ -C ₂	1.46775	1.47447	1.46976	1.47126	1.47609
C ₂ -C ₁	1.36745	1.3627	1.366	1.36494	1.36159
C ₁ -C _d	1.50370	1.50802	1.50265	1.50036	1.50009
HOMO	-0.13315	-0.13448	-0.13518	-0.13723	-0.14048
LUMO	-0.05488	-0.05551	-0.05743	-0.06021	-0.06403
HOMO-1	-0.18312	-0.18435	-0.18579	-0.18772	-0.19268
LUMO+1	-0.04014	-0.03912	-0.03790	-0.03587	-0.03204

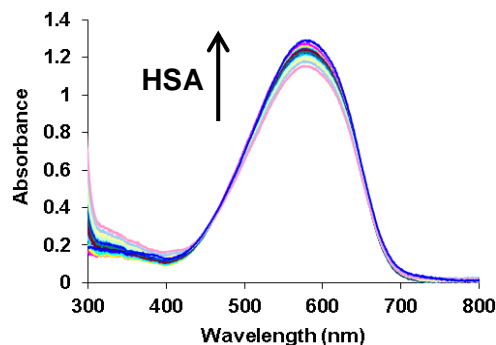


Figure S9: UV-vis spectra of probe **3** in H₂O buffered with HEPES, pH = 7.4 with the addition of human serum albumin (HSA).

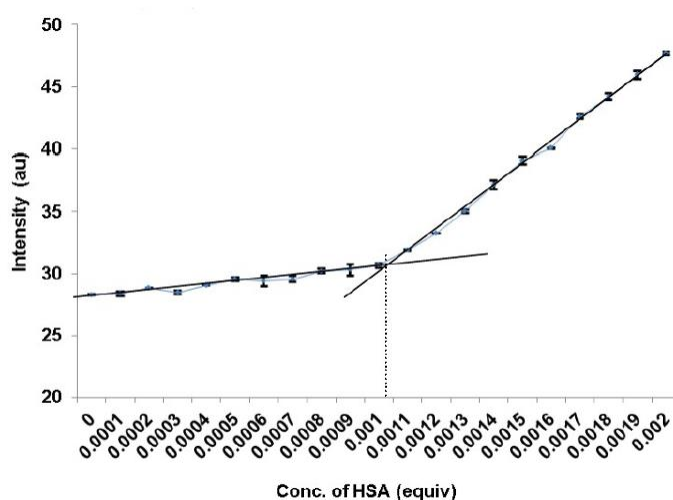


Figure S10a: Showing the fluorescence intensity of Probe **3** at 680 nm as a function of HSA concentration (equiv.) in H₂O buffered with HEPES, pH = 7.4, $\lambda_{ex} = 550$ nm.

To determine the detection limit, fluorescence titration of probe **3** with HSA was carried out by adding aliquots of HSA solution (in equiv.) and the fluorescence intensity as a function of HSA added was then plotted. From this graph the concentration at which there was a sharp change in the fluorescence intensity multiplied with the concentration of probe **3** gave the detection limit. Equation used for calculating detection limit (DL):

$$DL = CL \times CT$$

CL = Conc. of Ligand; CT = Conc. of Titrant at which change observed.

Detection limit (DL) of HSA with Probe **3**:

$$\text{Thus; } DL = 0.00107 \times 10^{-5}$$

$$= 10.7 \times 10^{-9}$$

$$= 10.7 \text{ nM}$$

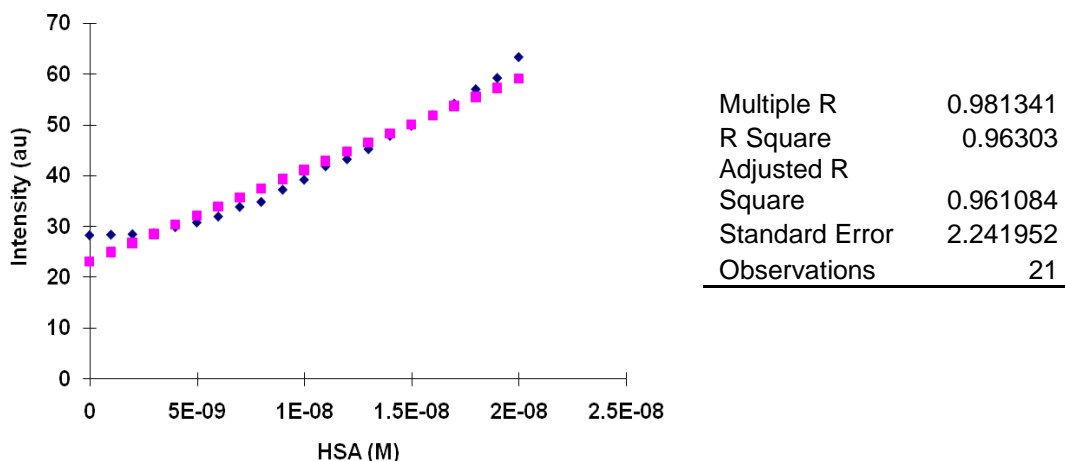


Figure S10b: Showing the fluorescence intensity of Probe **3** at 680 nm as a function of HSA concentration (equiv.) in H₂O buffered with HEPES, pH = 7.4, $\lambda_{\text{ex}} = 550$ nm.

The detection limit¹ was calculated based on the fluorescence titration. To determine the S/N ratio, the emission intensity of probe **3** without HSA was measured by 10 times and the standard deviation of blank measurements was determined. The detection limit is then calculated with the following equation:

$$DL = 3 \times SD/S$$

Where SD is the standard deviation of the blank solution measured by 10 times; S is the slope of the calibration curve.

From the graph we get slope (S) = 1797436.36, and SD value is 0.0062

Thus using the formula we get the Detection Limit (DL) = 10.03×10^{-9} M i.e. probe **3** can detect HSA in this minimum concentration through fluorescence method.

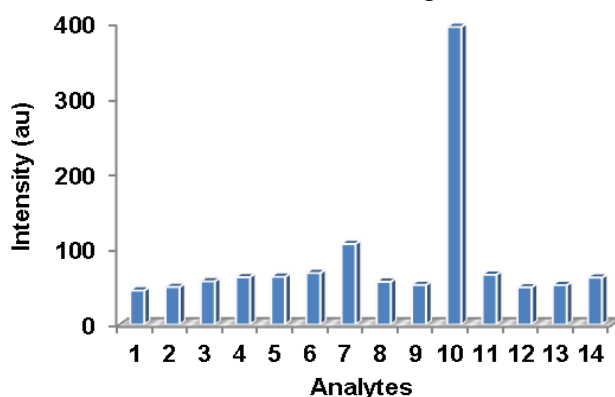


Figure S11: Fluorescence selectivity of probe **3** (10.0 μM) in the presence of various analytes (15 μM HSA and 60 μM for other analytes); 1 = glutathione reductase (GSSR), 2 = haemoglobin, 3 = trypsin, 4 = DNase, 5 = lysozyme, 6 = cysteine, 7 = BSA, 8 = homocysteine, 9 = glutathione, 10 = HSA, 11 = dithiothreitol, 12 = RNA (4 $\mu\text{g}/\text{ml}$), 13 = Glucose, 14 = ctDNA (5 $\mu\text{g}/\text{ml}$).

¹ S. Goswami, S. Das, K. Aich, D. Sarkar, T. K. Mondal, C. K. Quah, H.-K. Fun, *Dalton Trans.*, 2013, **42**, 15113.

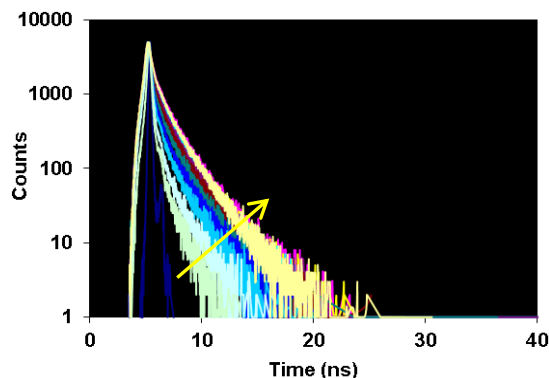


Figure S12: Fluorescence lifetime decay profiles of probe **3** in the presence HSA (15 μM) in H_2O buffered with HEPES, $\text{pH} = 7.4$. Sky green line is free probe **3** and yellow line corresponds **HSA-3** complex and blue line is IRF= instrument response function. $\lambda_{\text{ex}} = 635 \text{ nm}$ and emission spectra are recorded at 680 nm with 32 slit width.

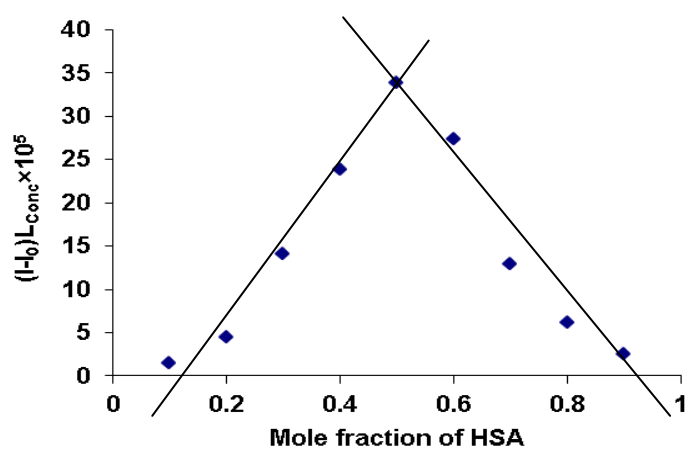


Figure S13: Job's plot for determining the stoichiometry (1:1) of probe **3**–HSA complexation.

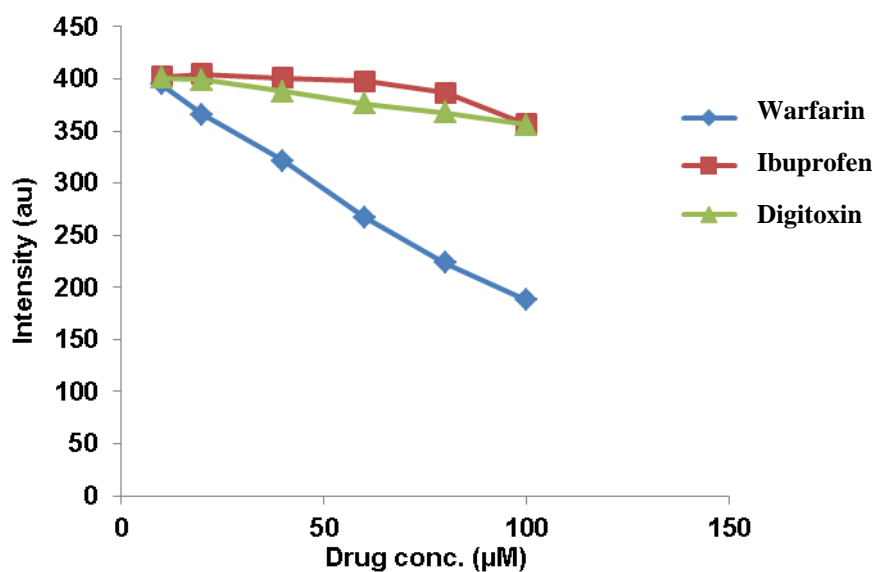


Figure S14: Displacement of probe **3** from **HSA-3** complex by addition of different site-specific drugs ($\lambda_{\text{ex}} = 550 \text{ nm}$ and $\lambda_{\text{em}} = 680 \text{ nm}$), warfarin, ibuprofen and digitoxin respectively.

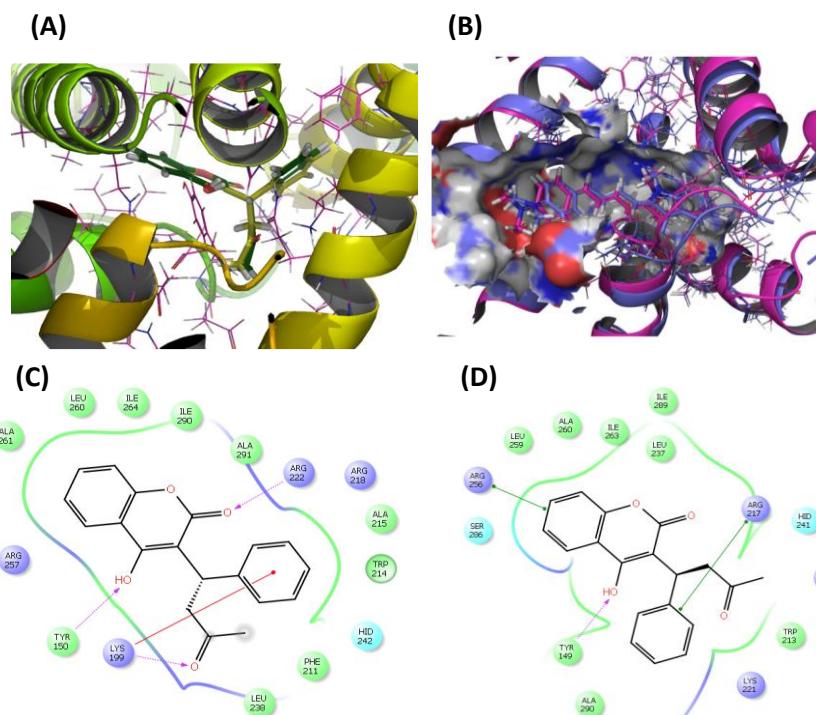


Figure S15: (A) Comparison of the HSA-warfarin complex in docked pose (green) and X-ray pose (yellow); (B) Superimposed HSA-Warfarin and BSA-warfarin complexes (alignment score 0.066, RMSD 1.26, pink for HSA and Blue for BSA); ligand-protein interaction plots of (C) warfarin at HSA site I; (D) warfarin at BSA site I

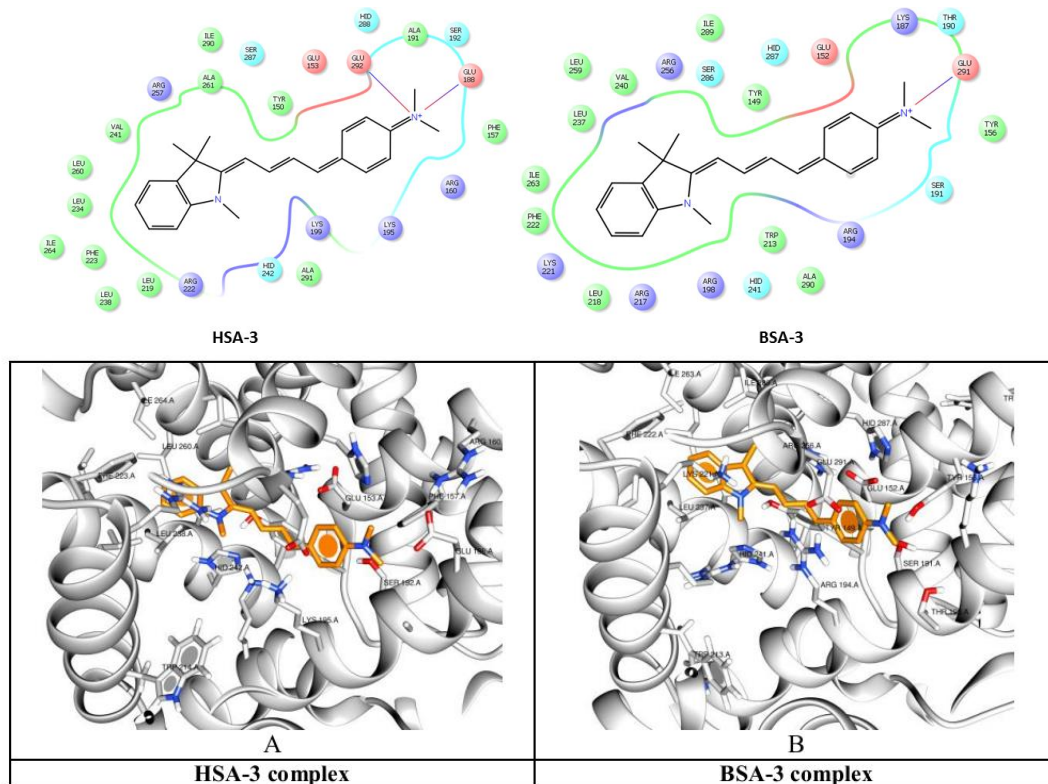


Figure S16: Docking poses for HSA-3 and BSA-3 complexes

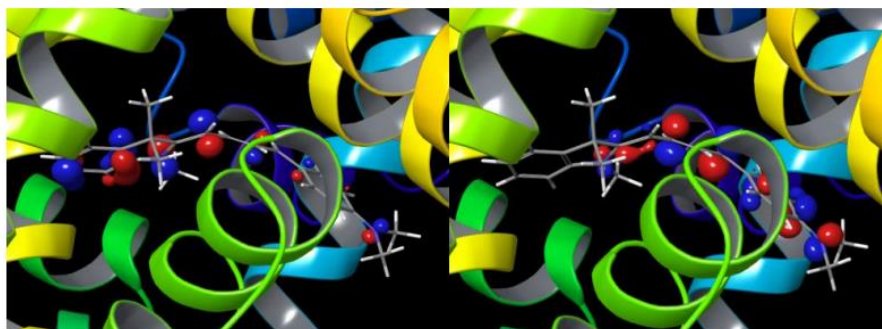


Figure S17: HOMO-LUMO using the ground state configuration in QM/MM protocol in HSA-probe complex (**DFT631G:OPLS2.1**)

HOMO = -0.115624au, HOMO-1= 0.14917au; HOMO-2=-0.160727au
 LUMO=-0.052122au; LUMO+1=0.038112au; LUMO+2=0.047760au

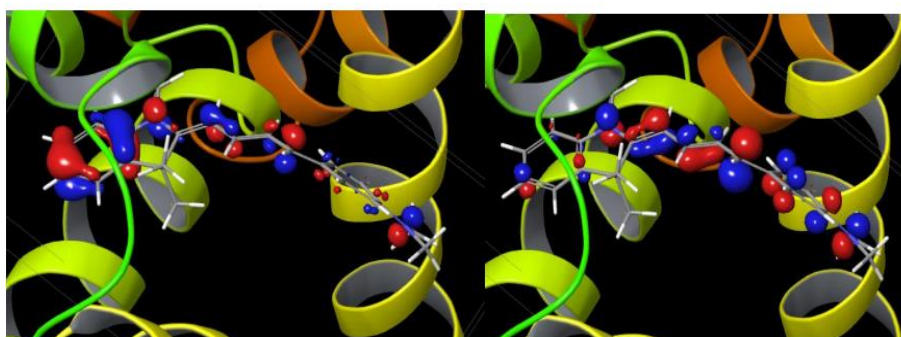


Figure S18: HOMO-LUMO using the ground state configuration in QM/MM protocol in BSA-probe complex (**DFT631G:OPLS2.1**)

HOMO= -0.222719au; HOMO-1=-0.244588au; HOMO-2=-0.276831au;
 LUMO=-0.176057au; LUMO+1=-0.103816au; LUMO+2=-0.089385au

Table S2: Output results of QM/MM calculation of both the proteins with the respective probes

	QM/MM energy	S (cal/mol/K, 298K)	Enthalpy (kcal/mol)	G	Total Energy
HSA-war	-1058.19	130.881	-11.156	-27.866	-1057.86
BSA-war	-1058.01	114.810	-9.359	-24.871	-1057.68
HSA-3	-1026.49	148.187	-14.009	-30.173	-1026.01
BSA-3	-1025.55	135.195	-12.185	-28.123	-1025.05

The ligand and protein preparation jobs were carried out in Schrodinger 2014 suite, for ligand preparation first diverse conformations were generated in ConfGen protocol using the OPLS 2005 at Distance-dependant electrostatic mode using the enhanced planarity of the conjugated pi groups using water as solvent, then the generated conformation were subjected to LigPrep protocol using the default settings at pH range of 7.0-2.0. Followed by the ligand preparation the obtained PDB files of HSA (2BXD, co-crystallised with warfarin) and BSA () the water molecules (except within 5.0Å^o range) and ligands were removed and subjected under the protein preparation wizard for pre-processing, modifying and refining. Thus obtained proteins were found with the RMSD of 1.26 and Alignment Score of 0.066 which than used for (i) Normal Glide docking then the best pose configuration were sorted on the

basis of minimum OPLS energy; (ii) Induced Fit Docking (IFD) protocols. Thus obtained best poses were subjected to the QM/MM calculation using the DFT/6-31G for the QM region and Amber for the Molecular mechanics region. The binding energies of the protein-ligand complexes were also calculated using the Molecular Mechanics/Generalized Born Surface Area (MM-PBSA) method following the equation $G_{\text{bind}}=G_{\text{(complex)}}+G_{\text{(P)}}+G_{\text{(L)}}$. The obtained optimised structure of the protein-ligand complexes were used for the calculation of the emission pattern which was carried out using the trimmed protein (Figure XX). The optimised structure thus obtained was subjected for the further trimming just to the extent containing the aromatic amino acid residues for the approximated prediction of the fluorescence enhancement.

The structure corroborating at the minimum energy was further optimised using the B3LYP/6-31G* basis set under trimmed protein environment (using NMA and Ac as the capping group prepared using the Maestro academic edition). The flexibility at the binding pocket was considered using the Induced fit docking method in the Glide docking protocol in the Schrodinger 2015 suite. The docking studies depicted that the probe under biological condition (pH 7.0-3.5) is capable of showing the salt-bridge interaction between the (dimethylaminophenyl) DMAP-Nitrogen atom and Glu-291 in BSA and 292, 188 in HSA in both the proteins the ligand was observed in transoid forms although during ligand preparation the possible geometrical isomers due to the rotation along C1_{linker}-C2_{indoline} and C2_{linker}-C3_{linker} was also considered but were not found showing effective results as shown in the docking results (Table 1 S1). The Induced fit docking was carried out and it was found that though the pocket captured with the probe in HSA was found slightly lesser than the BSA especially at the cross section residing the DMAP residues (Table CS area), in addition the free rotation in the respective pockets was found more restrictive in the case of the HSA as was analysed through the coordinate scan using the B3LYP/Lanl2mb.

Table S2.1: Cross-section contribution of different fragments of probe (3) in HSA and BSA protein at site I obtained through docking poses resulted after Induced fit docking protocol.

	HSA	BSA
Indoline	268.092	268.092
DMAP	336.631	359.945
linker	216.623	216.623
total	634.535	702.79

Table S2.2: Docking Results for the best rotamers obtained from the Normal glide docking in XP interaction mode. (The Probes was assumed to be capable of attaining the energy required or the geometrical isomerism for enabling a larger set of input structures which are similar so as to better detail about the protein-ligands interaction, the best obtained isomers are given below along reason of their discordance)

Title	Shape Sim	docking score	glide gscore	glide evdw	glide ecoul	glide emodel	glide energy
w	0.897	-6.705	-9.482	-45.723	-4.043	-55.819	-49.766
tt_1	0.537	-6.068	-6.075	-39.391	-2.907	-53.923	-42.298
cis-trans_1	0.572	-8.071	-8.078	-42.653	-3.764	-66.437	-46.417
i	0.398	-4.848	-8.694	-21.2	-11.532	-45.551	-32.732
cis-trans	0.614	-5.539	-5.545	-43.615	-3.362	-73.644	-46.977
cis-trans	0.614	-5.799	-5.805	-39.651	-2.134	-62.113	-41.786
tt_1	0.537	-5.128	-7.789	-41.761	-7.935	-62.435	-49.696

cis-trans	0.614	-8.349	-8.356	-45.982	-3.026	-65.618	-49.008
cis-cis	0.571	-8.477	-8.483	-38.688	-1.449	-61.953	-40.136
i	0.398	-4.345	-8.191	-28.164	-6.442	-47.776	-34.606
w	0.897	-5.541	-8.319	-41.736	-4.578	-69.938	-46.314
glide einternal	glide ligand efficiency	glide ligand efficiency sa	glide ligand efficiency ln	glide eff state penalty			
1.793	-0.292	-0.829	-1.621	2.777			
0.086	-0.243	-0.71	-1.438	0.007			
1.719	-0.323	-0.944	-1.913	0.007			
6.051	-0.323	-0.797	-1.307	3.846			
2.909	-0.222	-0.648	-1.313	0.007			
7.95	-0.232	-0.678	-1.374	0.007			
10.428	-0.205	-0.6	-1.216	2.66			
11.113	-0.334	-0.977	-1.979	0.007			
4.187	-0.339	-0.991	-2.009	0.007			
1.261	-0.29	-0.714	-1.172	3.846			
2.519	-0.241	-0.685	-1.34	2.777			
XP GScore	XP PhobEn	XP LowMW	XP RotPenal	XP LipophilicEvdW	XP Electro	XP Sitemap	
-9.482	-1.75	-0.472	0.25	-5.526	-0.303	-0.4	
-6.075	-0.2	-0.395	0.22	-5.659	-0.218	0	
-8.078	-1.148	-0.395	0.22	-6.209	-0.282	-0.265	
-8.694	-1.57	-0.5	0.499	-3.91	-0.865	0	
-5.545	-1.122	-0.395	0.22	-6.194	-0.252	-0.303	
-5.805	-1.5	-0.395	0.22	-6.172	-0.16	-0.299	
-7.789	-2.468	-0.392	0.219	-7.344	-0.595	-0.208	
-8.356	-0.923	-0.395	0.22	-7.737	-0.227	-0.294	
-8.483	-1.511	-0.395	0.22	-6.582	-0.109	-0.106	
-8.191	-1.633	-0.5	0.499	-4.529	-0.483	0	
-8.319	-1.562	-0.472	0.25	-5.837	-0.343	0	
Ionization Penalty	State Penalty	Potential Energy-OPLS-2005	glide lipo	glide rewards	glide erotb		
2.6049	2.7773	72.714	-2.604	-2.182	0.584		
0.0088	0.0067	191.893	-1.828	-1.392	0.514		
0.0088	0.0067	195.751	-2.794	-2.173	0.514		
3.6046	3.8459	41.251	-2.432	-2.412	1.163		
0.0088	0.0067	195.751	-2.697	-1.773	0.514		
0.0088	0.0067	195.751	-2.139	-2.257	0.514		
2.4955	2.6602	211.213	-2.881	-1.979	0.511		
0.0088	0.0067	195.751	-3.09	-2.021	0.514		
0.0088	0.0067	212.65	-1.851	-1.537	0.514		
3.6046	3.8459	41.251	-1.943	-2.227	1.163		
2.6049	2.7773	72.714	-1.753	-1.349	0.584		
Prime Coulomb	Prime Covalent	Prime vdW	Prime Solv GB	Prime Lipo	Prime Energy	Prime Hbond	
-17501.672	3036.924	-2170.326	-4625.256	-3013.828	-24829.8	-268.527	
-17446.65	3064.78	-2183.483	-4720.451	-3042.096	-24883	-268.809	
-17426.31	3072.389	-2158.69	-4728.387	-3036.979	-24831.7	-263.664	
-17497.519	3015.556	-2147.618	-4612.844	-3009.3	-24799.2	-263.764	
-17406.341	3060.206	-2176.567	-4739.858	-3044.263	-24854.4	-263.77	
-17396.697	3057.269	-2161.341	-4748.511	-3046.8	-24843	-263.746	
-17416.814	2806.039	-1896.825	-4786.733	-2987.159	-24827	-290.395	
-17447.59	2802.068	-1890.904	-4741.996	-2986.85	-24808.3	-290.323	
-17398.278	2803.21	-1872.731	-4780.575	-2979.153	-24773.8	-286.135	
-17554.208	2760.288	-1864.169	-4614.496	-2953.354	-24763	-288.955	
-17541.113	2762.931	-1869.787	-4602.897	-2950.752	-24742.8	-288.94	
Prime Packing		Prime SelfCont		IFDScore			
-21.844		-265.269		-1250.97			
-21.741		-264.523		-1250.22			
-24.93		-265.14		-1249.66			
-20.954		-262.783		-1248.66			
-20.289		-263.49		-1248.26			
-21.631		-261.504		-1247.95			
-25.289		-229.826		-1249.14			
-23.14		-229.567		-1248.77			
-29.066		-231.056		-1247.17			
-19.528		-228.555		-1246.34			
-21.823		-230.443		-1245.46			

Table S3: Qsite results using B3LYP/6-31G(d,p)

	HSA-3	BSA-3
Shape Sim	0.686	0.686
docking score	-3.986	-3.584
glide gscore	-3.986	-3.584
glide evdw	-29.433	-19.988
glide ecoul	1.139	-0.935
glide emodel	6.374	-23.942
glide energy	-28.294	-20.923
glide einternal	32.895	0
glide ligand efficiency	-0.159	-0.143
glide ligand efficiency sa	-0.466	-0.419
glide ligand efficiency ln	-0.945	-0.849
glide posenum	15	11
glide eff state penalty	0	0
XP GScore	-3.986	-3.584
XP PhobEn	-0.692	-1.297
XP LowMW	-0.395	-0.395
XP RotPenal	0.147	0.147
XP LipophilicEvdW	-3.464	-3.316
XP Electro	0.085	-0.07
XP PiStack	0	0
XP ExposPenal	0.333	0.348
QM/MM Energy	-1034.146629	-1033.892747
Zero Point Energy (kcal/mol)	305.563	303.73
Entropy (cal/mol/K, 298K)	139.437	138.992
Enthalpy (kcal/mol, 298K)	12.962	13.009
Free Energy (kcal/mol, 298K)	-28.611	-28.431
Total Internal Energy at 298.15K (au)	-1033.639971	-1033.388935
Total Enthalpy at 298.15K (au)	-1033.639027	-1033.38799
Total Free Energy at 298.15K (au)	-1033.705278	-1033.45403

Table S4: Results with the Trimmed proteins of the both BSA and HSA (capped using ACE and NMA)

	BSA-WAR	BSA-3	HSA-war	HSA-3
MMGBSA dG Bind(NS) Hbond	-0.821	0	-1.414	0
MMGBSA dG Bind(NS) Coulomb	-8.124	176.515	-20.455	128.412
MMGBSA dG Bind(NS) Packing	-1.473	-0.759	-1.492	0
MMGBSA dG Bind(NS) Lipo	-38.4	-61.22	-33.783	-57.877
MMGBSA dG Bind(NS)	-80.072	-84.757	-77.47	-81.42
MMGBSA dG Bind(NS) Solv GB	16.29	-143.386	18.018	-101.818
MMGBSA dG Bind(NS) vdW	-47.543	-55.907	-38.345	-50.138
Rec Strain Hbond	-1.631	-2.331	-0.077	-0.032
Rec Strain Coulomb	6.344	-16.756	-2.591	0.272
Rec Strain Covalent	3.238	10.348	-0.905	4.067
Rec Strain Packing	4.021	4.675	-0.115	0.587
Rec Strain Lipo	-3.06	-2.741	-0.414	-0.021
Rec Strain Energy	-2.65	-0.981	-3.699	3.313
Rec Strain Solv GB	-13.254	4.856	1.111	-3.232
Rec Strain vdW	1.594	1.549	-0.625	2.069
Rec Strain SelfCont	0.098	-0.581	-0.084	-0.397
MMGBSA dG Bind SelfCont	0.098	-0.581	-0.084	-0.397
Prime Coulomb	-17589.322	-17420.731	-17656.2	-17493.527
Prime Covalent	4978.713	5022.272	3118.661	3158.089
Prime vdW	2589.303	2579.765	5081.709	5074.842
Prime Solv GB	-4700.988	-4914.594	-4662.51	-4860.709
Prime Lipo	-3030.25	-3060.307	-2978.28	-3008.889
Prime Energy	-18261.6	-18301.9	-17598.1	-17628.3
Prime Hbond	-241.47	-241.35	-265.622	-264.163
Prime Packing	-22.637	-21.269	-21.825	-19.632
Prime SelfCont	-244.97	-245.649	-214.026	-214.34

Table 4.1: The MMGBSA and MMGHSA binding results for the system comprising warfarin complex

	Ligand Energy	Complex Energy	Solvation Energy	Prime Energy	Prime Solv GB	Receptor Solv GB	Receptor Solv GB
BSA-warfarin complex	9.23	-17598.1	-4662.534	-17598.1	-4662.534	-4675.17	-4675.17
BSA-3	-28.318	-17628.328	-4860.709	-17628.3	-4860.709	-4675.17	
	Ligand Energy	Complex Energy	Solvation Energy	Prime Energy	Prime Solv GB		Receptor Solv GB
HSA-warfarin complex	14.508079	-18239.55457	-4715.260824	-18239.55457	-4715.260824	-4675.17	-4696.68
HSA-3 complex	-23.09266	-18301.86387	-4914.594037	-18301.86387	-4914.594037	-4675.17	

Table S5: Results of the trimmed protein optimization

BSA-WAR complex optimization RB3LYP631G:RHF321G:AMBER

	(Hartree/Particle)
Zero-point correction=	0.215621
Thermal correction to Energy=	0.22626
Thermal correction to Enthalpy=	0.227204
Thermal correction to Gibbs Free Energy=	0.177993
Sum of electronic and zero-point Energies=	-1021.418653
Sum of electronic and thermal Energies=	-1021.408014
Sum of electronic and thermal Enthalpies=	-1021.40707
Sum of electronic and thermal Free Energies=	-1021.456281

HSA-WAR complex optimization RB3LYP631G:RHF321G:AMBER

Zero-point correction=	0.247743
Thermal correction to Energy=	0.259344
Thermal correction to Enthalpy=	0.260288
Thermal correction to Gibbs Free Energy=	0.208907
Sum of electronic and zero-point Energies=	-1021.425679
Sum of electronic and thermal Energies=	-1021.414078
Sum of electronic and thermal Enthalpies=	-1021.413134
Sum of electronic and thermal Free Energies=	-1021.464516

BSA-3 complex optimization RB3LYP631G:RHF321G:AMBER

Zero-point correction=	0.27587
Thermal correction to Energy=	0.289406
Thermal correction to Enthalpy=	0.29035
Thermal correction to Gibbs Free Energy=	0.233544
Sum of electronic and zero-point Energies=	-989.7895617
Sum of electronic and thermal Energies=	-989.7760257
Sum of electronic and thermal Enthalpies=	-989.7750817
Sum of electronic and thermal Free Energies=	-989.8318877

HSA-3 complex optimization RB3LYP631G:RHF321G:AMBER

Zero-point correction=	0.274271
Thermal correction to Energy=	0.288171
Thermal correction to Enthalpy=	0.289115
Thermal correction to Gibbs Free Energy=	0.230219
Sum of electronic and zero-point Energies=	-989.7888286
Sum of electronic and thermal Energies=	-989.7749286
Sum of electronic and thermal Enthalpies=	-989.7739846
Sum of electronic and thermal Free Energies=	-989.8328796

BSA-3 (trimmed having the aryl substituents)

Zero-point correction=	0.002673 (Hartree/Particle)
Thermal correction to Energy=	0.002833
Thermal correction to Enthalpy=	0.003777

Thermal correction to Gibbs Free Energy=	0.041192
Sum of electronic and zero-point Energies=	-5369.857635
Sum of electronic and thermal Energies=	-5369.854802
Sum of electronic and thermal Enthalpies=	-5369.853858
Sum of electronic and thermal Free Energies=	-5369.898827

HSA-3 (trimmed having the aryl substituents)

Zero-point correction=	0.002631 (Hartree/Particle)
Thermal correction to Energy=	0.002833
Thermal correction to Enthalpy=	0.003777
Thermal correction to Gibbs Free Energy=	0.041401
Sum of electronic and zero-point Energies=	-5539.909437
Sum of electronic and thermal Energies=	-5539.906604
Sum of electronic and thermal Enthalpies=	-5539.90566
Sum of electronic and thermal Free Energies=	-5539.950837

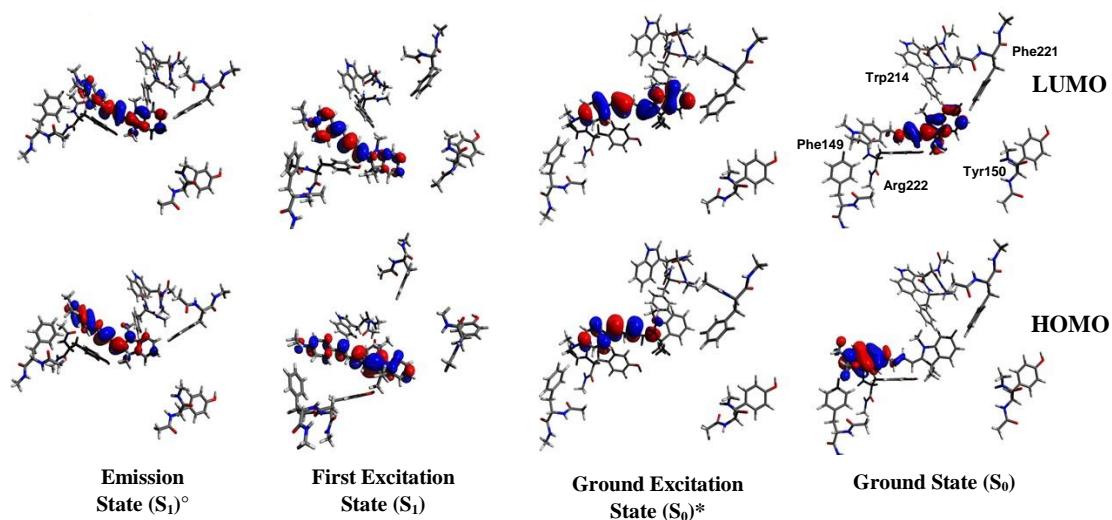


Figure S19: Different states of **HSA-3** complex used for the calculation of reorganization energy.

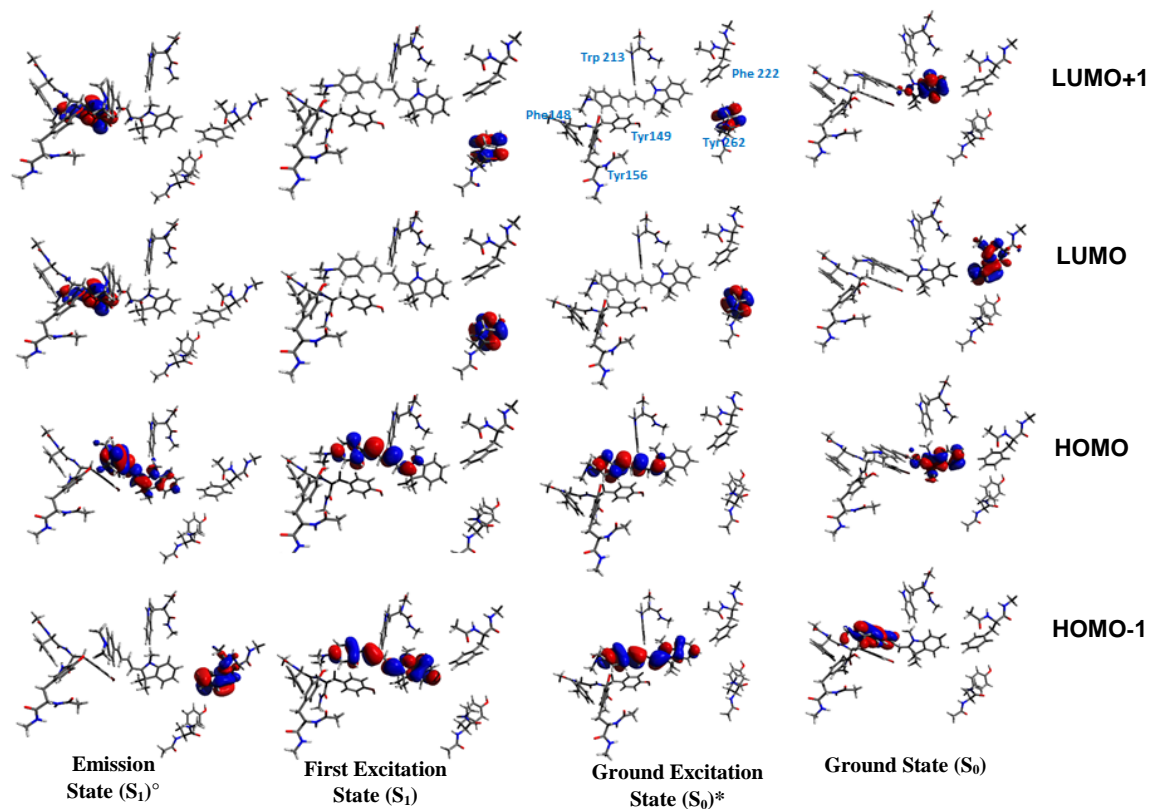


Figure S20: Different states of **BSA-3** complex used for the calculation of reorganization energy.

Table S6: Calculation of Reorganisation energy using $\lambda_s = [(S_0^g) - (S_0^e)] + [(S_1^g) - (S_1^e)]$

HSA-3 complex	SPE (au)	λ_s (au)	BSA-3 complex	SPE (au)	λ_s (au)
(S_0^g)	-2483.81	0.1252	(S_0^g)	-2612.92	0.11447
(S_1^g)	-2483.68		(S_1^g)	-2612.81	
(S_1^e)	-2483.81		(S_1^e)	-2612.92	
(S_0^e)	-2483.81		(S_0^e)	-2612.92	
(S_0^g)	-5369.857635	0.0000516	(S_0^g)	-5539.909437	0.000051
(S_1^g)	-5370.0060104		(S_1^g)	-5540.070608	
(S_1^e)	-5370.006062		(S_1^e)	-5540.070659	
(S_0^e)	-5369.857635		(S_0^e)	-5539.909437	

(S_0^g) optimized ground state(dft); (S_1^g) vertical excitation at ground state(td-dft); (S_1^e) optimized excited state (td-dft); (S_0^e) relax at excited state. λ_s = Reorganization energy of singlet state; SPE = Single point energy

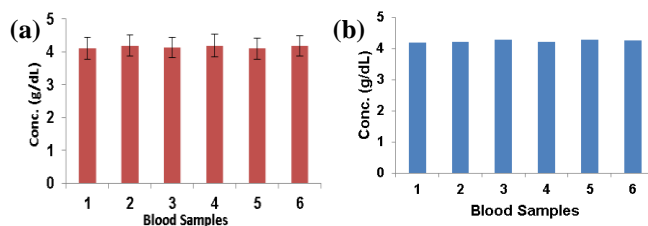


Figure S21: Data obtained for the HSA level using probe 3 in six different samples (normal blood samples); (b) data obtained from clinical laboratory using the standard procedure.

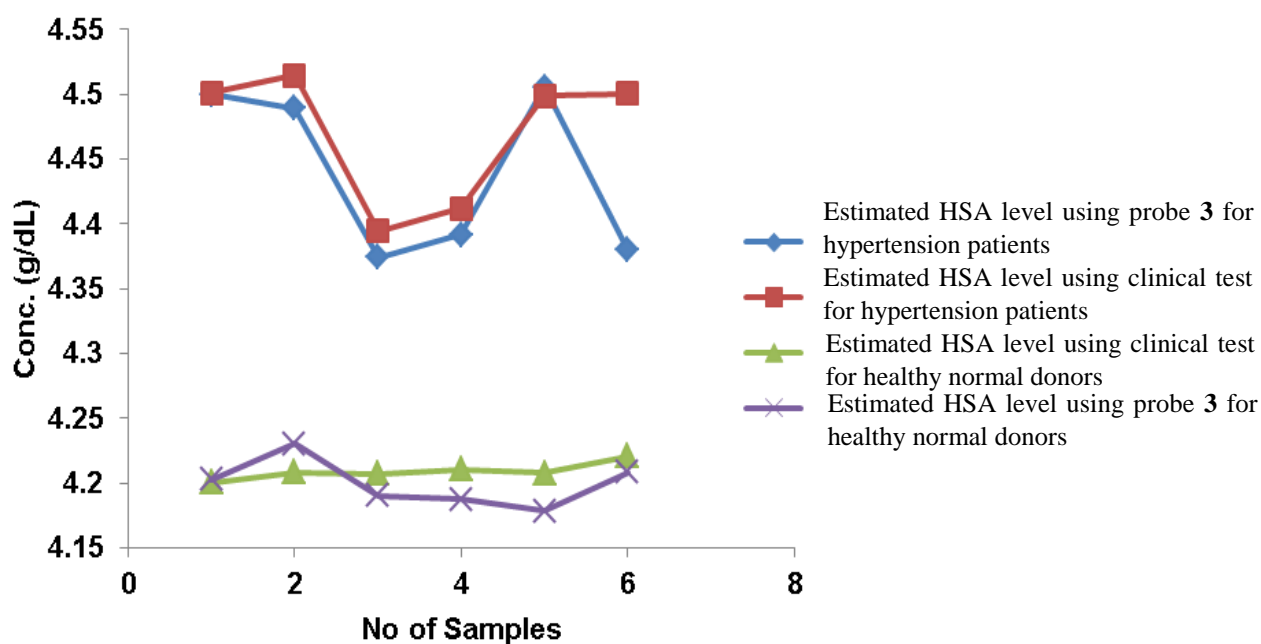


Figure S22: Data obtained for HSA level using probe 3 in six different samples comprising of normal and hypertension blood samples from fluorometric assay as well as clinical data.